JOURNAL OF SOLID STATE CHEMISTRY 116, 321–328 (1995)

New Thallium Oxycarbonates Built Up from Rock Salt Layers: $A_4Tl_2CO_3O_6$ (A = Ca, Sr, Ba)

V. Caignaert, M. Hervieu, F. Goutenoire, and B. Raveau

Laboratoire CRISMAT, ISMRA et Université de Caen Boulevard du Maréchal Juin, 14050 Caen Cédex, France

Received August 3, 1994; in revised form November 3, 1994; accepted November 9, 1994

The investigation of the systems AO–Tl_2O_3–ACO_3 has allowed three new oxycarbonates $A_4Tl_2CO_3O_6$ to be synthesized for A = Ca, Sr, Ba. A study of the system SrO–Tl_2O_3, under the same conditions, i.e., in sealed tubes, has not been able to detect the well-known oxide $Sr_4Tl_2O_7$. An XRD and ED study of these oxycarbonates leads to a tetragonal I-centered cell with $a \approx 5$ Å and $c \approx 18$ Å, previously obtained for $Sr_4Tl_2O_7$. The detailed ED study of the oxycarbonate $Ca_4Tl_2CO_3O_6$ has shown the following features: (i) there exist very weak extra reflections leading to an orthorhombic supercell $a' = 2a$, $b' = a$, $c' = c$, and (ii) streaks are observed along c* correlated to a disordered stacking of some (001) layers. The powder XRD and HREM investigation of this phase shows that its structure consists of distorted rock salt-type layers interleaved with layers of carbonate groups. The close relationships between this structure and that of the 1201 layered cuprates are discussed.

INTRODUCTION

The recent investigations of superconducting copper-based oxycarbonates have shown the great ability of thallium-based systems to form such compounds. This is indeed the case of the superconductors $Tl_{0.5}Pb_{0.5}Sr_4Cu_2CO_3O_6$ (1) and $TlBa_2Sr_2Cu_2CO_3O_6$ (2). Moreover, in the course of these syntheses performed in the presence of a CO_2 pressure, it was noted that the phase $Sr_4Tl_2O_7$, discovered by Schenck and Müller-Buschbaum (3) was, most of the time, more easily formed than without carbonates. These results suggest that the noncopper elements, especially thallium and strontium, may also be susceptible to generating oxycarbonates. The understanding of their chemistry is of prime importance, if one wants to control the chemical synthesis and optimization of the copper-based oxycarbonates. For this reason we have reconsidered the system SrO–Tl_2O_3, and we have investigated the systems AO–Tl_2O_3–ACO_3 for A = Ca, Sr, Ba. The present work deals with the synthesis and structural study of three new isotypic oxycarbonates $A_4Tl_2CO_3O_6$ with A = Ca, Sr, Ba, with an original structure built up from distorted rock salt-type layers interleaved wtih layers of carbonate groups.

EXPERIMENTAL

Neutron powder diffraction data were collected on the D2b diffractometer at the ILL, Grenoble. The compound was loaded in a vanadium can and data registered at room temperature with a neutron wavelength of 1.5940 Å over an angular range of 160° in 2θ. X ray powder diffraction data were collected either on a Seifert diffractometer using strictly monochromatized $CuK_{\alpha 1}$ or with a Philips diffractometer $CuK_{\alpha 1,2}$. The profile refinements were performed with the program Fullprof (4) that allows the full pattern decomposition and/or the Rietveld refinement of powder diffraction data. The electron diffraction study of the microcrystals was performed with a JEOL 200CX electron microscope fitted with a eucentric goniometer (±60°). The HREM study was performed with a TOPCON 002B electron microscope operating at 200 k V. The infrared transmittance spectra were measured between 400 and 4000 cm^{-1} using pellets of KBr containing 1/200 part of finely ground sample.

EVIDENCE FOR THE CARBONATION OF THE $Sr_4Tl_2O_7$ STRUCTURE: SYNTHESIS OF NEW OXYCARBONATES $A_4Tl_2CO_3O_6$ WITH A = Ca, Sr, Ba

In order to prepare $Sr_4Tl_2O_7$, mixtures of SrO_2 and Tl_2O_3 were heated at 650°C for 8 h in sealed silica tubes. Attempts to prepare this phase with the ideal stoichiometry, i.e., $SrO_2/Tl_2O_3 = 4$, lead always to a multiphasic sample. The best results, from the X ray diffraction (XRD) analysis, were obtained for an excess of SrO_2, i.e., for $SrO_2/Tl_2O_3 \approx 5$. Under these conditions, 10 g of a crystallized yellow powder could be prepared for a preliminary neutron diffraction study.

0022-4596/95 $6.00

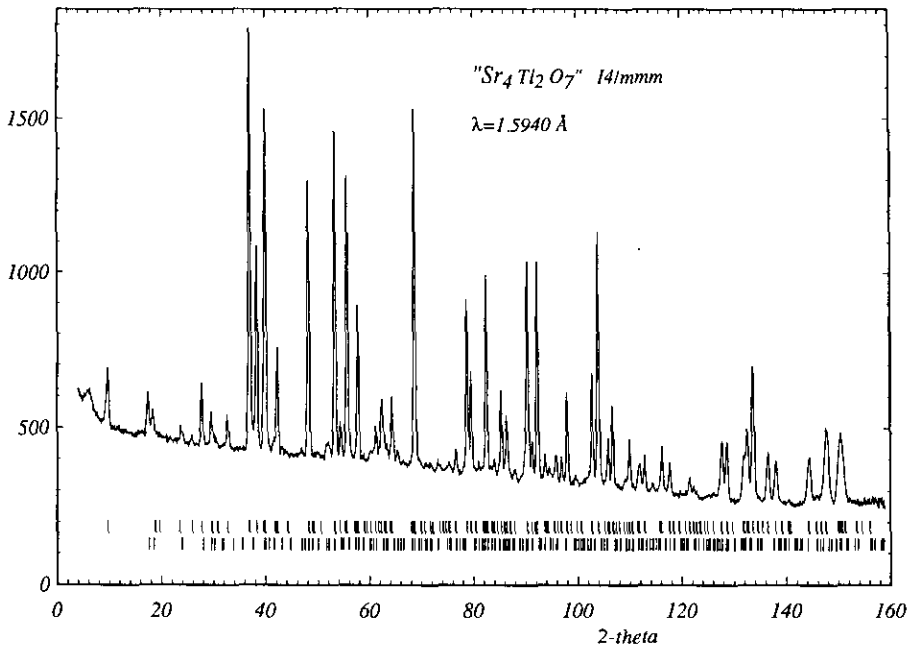

FIG. 1. Neutron diffraction pattern of $Sr_4Tl_2O_6CO_3$. The position of the Bragg peaks are indicated by the vertical marks. The bottom marks are those of $Sr(OH)_2$.

All the main reflections of the powder neutron diffraction pattern (Fig. 1) could be indexed in a tetragonal cell with $a = 5.02$ Å and $c = 18.63$ Å, previously established from the single crystal XRD study of $Sr_4Tl_2O_7$ (3). Nevertheless, $Sr(OH)_2$ as an impurity was detected on the ND pattern. Attempts to solve the structure in the space group $P4_2nm$, given by Schenck and Müller-Buschbaum or in the most symmetric space group $P4_2/mnm$, gave R_i factors above 20%. Moreover refinements of the variable parameters resulted in an abnormally high thermal factor for the oxygen site located at 0.25 0.25 0.25 in the latter space group. The refinement of the occupancy factor of this site and the Fourier diffrence maps both revealed a significant excess of scattering density at the $z = 0.25$ level, i.e., between the calcium oxygen layers (Fig. 2); the latter excess was found to be incompatible with an oxide of the system Tl–Sr–O since it would imply the presence of Tl(IV). In any case, the quality of our ND data did not allow any satisfactory refinement of the structure to be carried out.

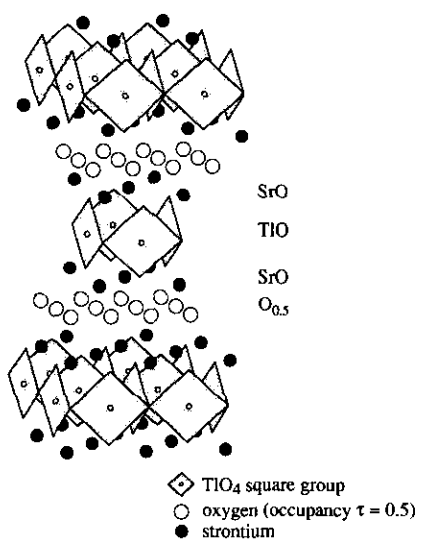

FIG. 2. Crystal structure of $Sr_4Tl_2O_7$.

The electron diffraction (ED) study performed on the same sample confirmed the above cell parameters. A subcell showing strong reflections with $a_s = 3.5$ Å and $c_s = 9.3$ Å (s = subcell) is clearly evidenced on the [110] ED pattern (Fig. 3) of this phase. However the systematic presence of extra reflections implies a true cell with $a = \sqrt{2}a_s \approx 5.0$ Å and $c = 2c_s \approx 18.7$ Å, corresponding to a I-type symmetry. In fact, for most of the crystals, modulated streaks were observed along $\mathbf{c}^*$ with maxima for h and $l = 2n + 1$ (small white arrow in Fig. 4a). These observations suggest a high degree of disorder in the stacking of the (001) atomic layers along $\mathbf{c}$ and explain the difficulty to solve correctly this structure from ND data.

The synthesis of $Sr_4Tl_2O_7$ was reconsidered, starting from 4 SrO and Tl_2O_3 mixed in a glove box. The mixture was heated in sealed silica tubes at 650°C for 8 hr. For this experimental method no phase with the $Sr_4Tl_2O_7$-type structure could be detected. At this stage of the

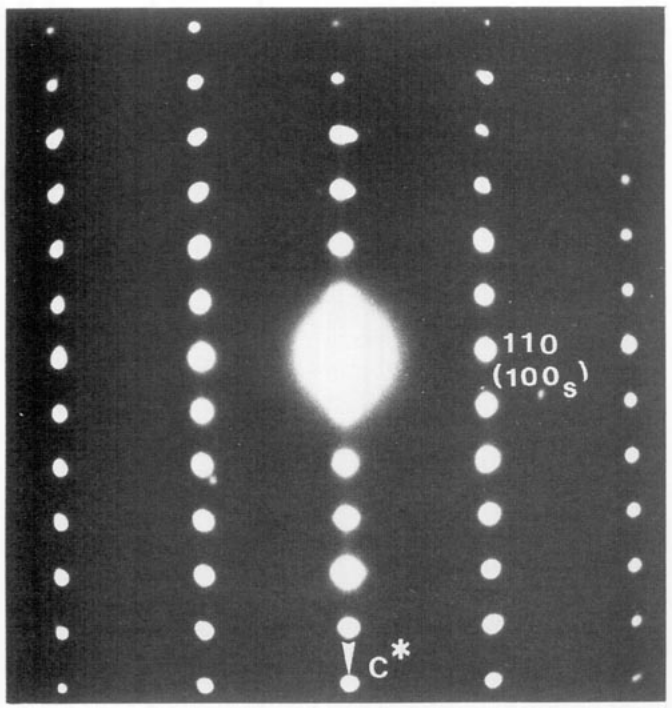

FIG. 3. $Sr_4Tl_2O_7$ [110] ED pattern. The strong reflections evidence a tetragonal subcell with a_s = 3.5 Å and c_s = 9.3 Å ("s" refers to the subcell).

study, the presence of alien ions such as hydroxyl or carbonate ions was considered as the starting material SrO_2 always contains $Sr(OH)_2$ and $SrCO_3$. The infrared analysis of the sample used in the ND study confirmed the presence of OH^- groups due to a small amount of $Sr(OH)_2$. But the most striking feature deals with the presence of CO_3^{2-} groups, with a rather high content compared to OH^- groups. These carbonates were introduced by the small amount of $SrCO_3$ contained in SrO_2. This latter fact suggest that the excess of strontium peroxide used in the precursor was necessary in order to increase the carbonate amount in the sample.

Thus the stabilization of such a phase was attributed to the presence of carbonate groups in the structure. The synthesis of oxycarbonates of the alkaline earth series, $A_4Tl_2CO_3O_6$ with A = Ca, Sr, Ba, was undertaken according to the above composition. We started from the mixtures of ACO_3, $3AO$, and Tl_2O_3 and used a glove box to avoid hydrolysis or hydration. By heating these mixtures in sealed silica tubes at 650°C, single phases were synthesized, with powder XRD patterns similar to that of $Sr_4Tl_2O_7$ (3), as shown from Fig. 5. Note also that, similarly to the strontium phase, all attempts to prepare $Ca_4Tl_2O_7$ or $Ba_4Tl_2O_7$ starting from CaO or BaO failed. The indexation of the powder XRD pattern of these new oxycarbonates made possible a tetragonal cell with parameters similar to those of $Sr_4Tl_2O_7$ as shown for in-

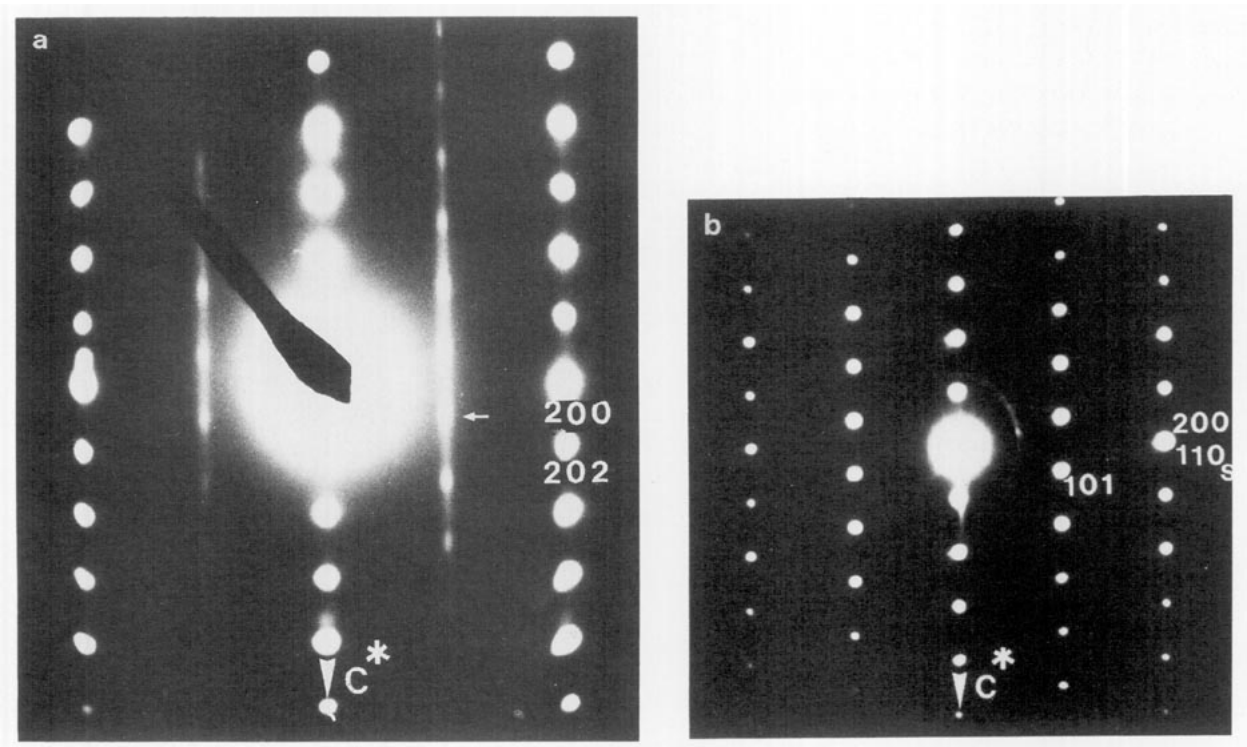

FIG. 4. (a) $Sr_4Tl_2O_7$ [010] ED pattern. Streaks are observed along c^* with only nodes for the odd h and l extra reflections (101 reflection is shown by a small white arrow). (b) $Ca_4Tl_2O_6CO_3$: typical ED pattern. Note that the extra reflections, such as 101, are strong with regards to the subcell reflections (subscript s).

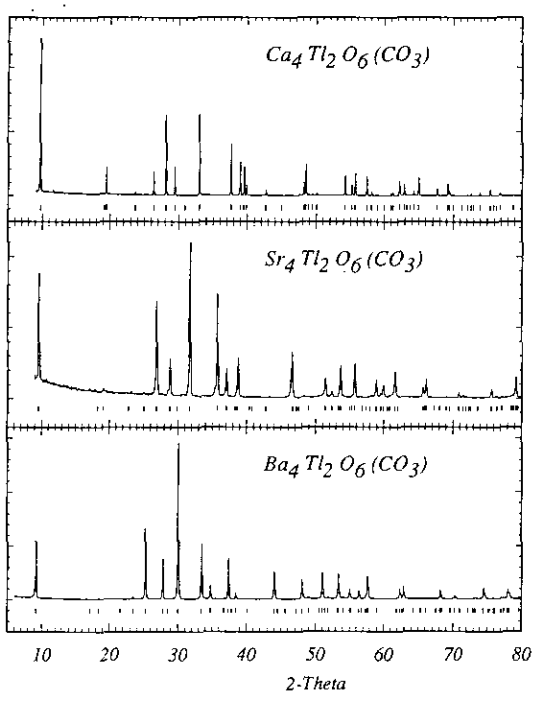

FIG. 5. XRD patterns of $Ca_4Tl_2CO_6CO_3$, $Sr_4Tl_2O_6CO_3$, and $Ba_4Tl_2O_6CO_3$. The marks under the patterns indicate the position of the Bragg reflections in the *I4/mmm* space group.

stance for $Ca_4Tl_2CO_3O_6$ (Table 1). The cell parameters increase significantly as the size of the alkaline earth cation increases.

HREM AND XRD STUDY OF THE OXYCARBONATE $Ca_4Tl_2CO_3O_6$

ED and HREM studies. Calcium, owing to its much smaller atomic number compared to strontium or barium, should allow a better location of oxygen and consequently of the CO_3^{2-} groups, from powder XRD structure refinement. Moreover, the preliminary ED study of the calcium phase showed a better ordering than for the two other oxycarbonates. Thus a systematic structural study of the new oxycarbonate $Ca_4Tl_2CO_3O_6$ was undertaken.

The ED investigation of $Ca_4Tl_2CO_3O_6$ showed that all the crystals exhibit a true cell with $a = \sqrt{2}a_s \approx 4.8$ Å and $c = 2\,c_s \approx 18.2$ g Å in agreement with the indexation of the powder XRD pattern, similarly to $Sr_4Tl_2CO_3O_6$. Nevertheless the extra reflections with respect to the subcell "s" ($a_s \approx 3.4$ Å, $c_s \approx 9.1$ Å) are very strong compared to $Sr_4Tl_2CO_3O_6$ (Fig. 4b). Note also that the reconstructions of the reciprocal space evidence the reflection conditions hkl, $h + k + l = 2n$, which imply a I-type symmetry for $Sr_4Tl_2CO_3O_6$ and for $Sr_4Tl_2O_7$ (3). Thus the $P4_2nm$ group used by Schenck and Müller-Buschbaum to solve the structure of $Sr_4Tl_2O_7$ appears artificial. Moreover the intensity of the extra reflections indicates that the ordering responsible for the supercell is well established. Diffuse streaks along **c*** related to the degree of disordering of the stacking of (001) layers are also observed, as in $Sr_4Tl_2CO_3O_6$. However the intensity of such streaks is much weaker than for the Sr phase.

TABLE 1
Subcell Parameters of $A_4Tl_2CO_3O_6$ (A = Ca, Sr, Ba)

	Ca	Sr	Ba
a_s (Å)	3.380	3.547	3.788
c_s (Å)	9.107	9.339	9.624
V_s (Å^3)	104.0	117.5	138.1
c_s/a_s	2.69	2.63	2.54

Note. The subscript "s" refers to the subscell (see text).

In fact the true symmetry of this phase is orthorhombic. A second set of very weak extra reflections appear in different sections of the reciprocal space; they are barely visible on the [001] ED patterns, due to their elongated shape along **c*** (Fig. 6b), but can be clearly observed by a tilting around **a***. These weak extra spots lead to the orthorhombic supercell $a' = 2a = 2\sqrt{2}a_s$, $b' = a = \sqrt{2}a_s$, $c' = c = 2c_s$ (Fig. 6a). Moreover, a (110) twinning is systematically observed, producing a pseudo-fourfold symmetry in the [001] ED patterns as shown from the schematic drawing in Fig. 6a. In the reciprocal space, the reflections are streaky, resulting in diffuse lines along **c*** which are sometimes hardly visible. This suggests the existence of an ordering phenomenon in the (001) plane and a high disorder along **c***. The fact that such weak extra spots correspond to streaks along **c*** does not allow the corresponding space group to be found out.

The high resolution electron microscopy study was performed in order to understand the origin of the superstructures. Although they are less sensitive to the electron beam than the $Sr_4Tl_2CO_3O_6$ phase, the crystals of the Ca phase are transformed after a few minutes exposure, so that a complete HREM observation is difficult. Nevertheless the [010] HREM images provide important information about the stacking of the cationic layers along **c**. Triple rows of white dots running along **a** are clearly visible (Fig. 7a, black arrow). They can easily be identified with $[CaO]_\infty$ and $[TlO]_\infty$ layers, according to the stacking sequence CaO–TlO–CaO similar to the SrO–TlO–SrO sequence proposed for $Sr_4Tl_2O_7$ (Fig. 2). Between these triple rows, one observed single rows where one dark dot alternates with one gray dot (curved arrows). Two successive single rows are shifted **a**/2 with respect to each other, leading to a centered cell. Such single rows contain the oxygen atoms, but may also contain the carbonate groups. Simulated images have been

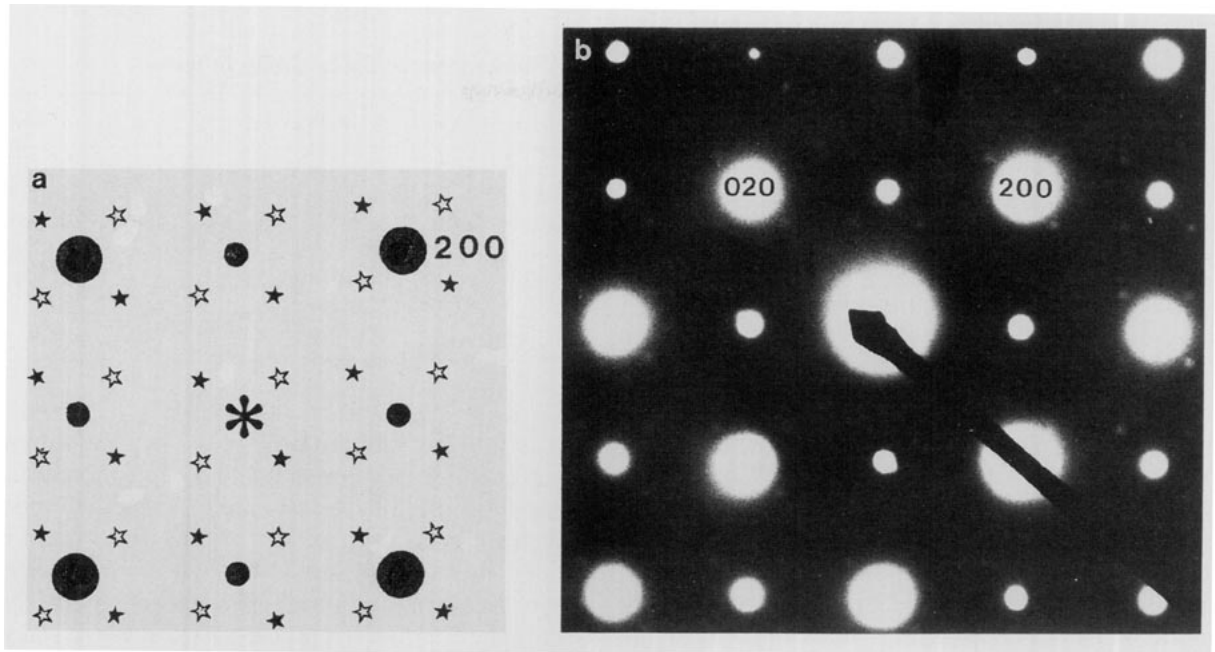

FIG. 6. $Ca_4Tl_2O_6CO_3$. (a) Schematic drawing of the [001] ED pattern; the extra reflections belong to two superposed 90° oriented systems represented by black and white stars. Each system corresponds to an orthorhombic cell with $a' = 2a$ and $b' = a$. (b) [001] ED pattern showing the weak extra reflections.

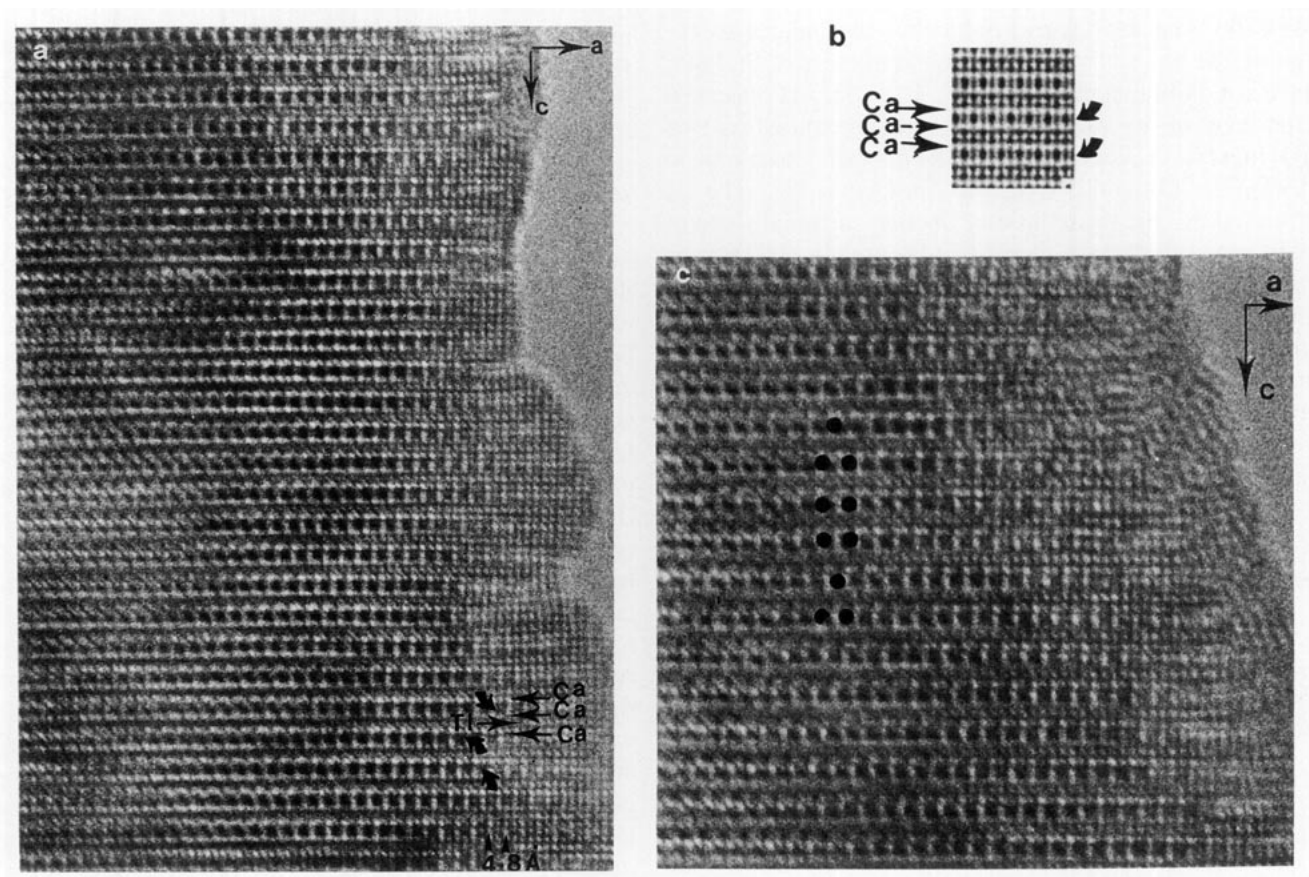

FIG. 7. $Ca_4Tl_2O_6CO_3$. (a) [101] HREM image; the nature of the cations is indicated and the oxygen–carbon rows are indicated by curved arrows. (b) Calculated image for a focus value of 20 nm and a crystal thickness of 28 Å. (c) [010] image of a defective area. Dark circles are added to show the absence of translation in three adjacent slices.

TABLE 2
Atomic Positions Deduced from the Patterson and Fourier maps in Space Group *I4/mmm*

	Model I		Model II		Model III		Model IV	
Thallium sites	4c	0, 1/2, 0	2a	0, 0, 0	4d	0, 1/2, 1/4	4e	0, 0, z = 0.25
			2b	0, 0, 1/2				
Calcium sites	4e	0, 0, z = 0.14	8g	0, 1/2, z = 0.14	4e	0, 0, z = 0.11	8g	0, 1/2, z = 0.11
	4e	0, 0, z = 0.36			4e	0, 0, z = 0.39		
Oxygen sites	2a	0, 0, 0	4c	0, 1/2, 0	4e	0, 0, z = 0.25	4d	0, 1/2, 1/4
	2b	0, 0, 1/2	4e	0, 0, z = 0.12	8g	0, 1/2, z = 0.13	4e	0, 0, z = 0.13
	8g	0, 1/2, z = 0.12	4e	0, 0, z = 0.38			4e	0, 0, z = 0.37

calculated with the positional parameters refined from the XRD pattern (see next paragraph), for different crystal thicknesses and focus values. Keeping in mind that these results only correspond to an average structure and that carbon and oxygen positions have to be carefully refined from neutron diffraction data, the calculated images confirm our observations: for a focus value of 20 nm the rows of cations appears as rows of bright dots and the oxygen–carbon layers exhibit a strong variation in the dot brightness, with a 4.5-Å periodicity between the dark and the gray dots (Fig. 7b); this feature is translated by **a**/2 in the adjacent layers. Note that the images calculated on the basis of the structure parameters of $Sr_4Tl_2O_7$ (3) do not exhibit such a contrast. The contrast observed at the level of the carbonate groups, surrounded by two CaO layers, is very different from that observed in $A_2CuO_2CO_3$ (5) and $Tl_{0.5}Pb_{0.5}Sr_4Cu_2CO_3O_6$ (1). This is correlated to the orientations of the carbonate group which are different in $Ca_4Tl_2CO_3O_6$ and in the copper oxycarbonates. Thus the HREM observations confirm that the stacking of the cationic layers along **c** can be compared to that observed for $Sr_4Tl_2O_7$, i.e., CaO–TlO–CaO ... CaO–TlO–CaO. It also supports the view point that the structure should be solved in a centered space group, but neither shows nor implies the presence of carbonate groups. The HREM study shows a second interesting feature: in some areas (Fig. 7c), three successive single rows (see black dots) are no longer shifted along **a** with respect to each other, so that the c parameter is divided by two, i.e., equal to 9 Å. This shows that the single "oxygen–carbonate" layer can be translated **a**/2 with respect to the triple $[Ca_2TlO_3]_\infty$ layers. The random translation of the "oxygen–carbonate" layers with respect to the triple $[Ca_2TlO_3]_\infty$ layers explains the diffuse streaks that are observed along **c***.

TABLE 3
Atomic Positions for $Ca_4Tl_2CO_3O_6$ (Space Group *I4/mmm*): a = 4.77944(4) Å, c = 18.2111(2) Å R_{wp} = 15.0%, R_e = 6.38%, χ^2 = 5.5, R_i = 4.18%

Sites		x	y	z	B	τ
Tl	4e	0	0	0.25268(7)	0.54(2)	4
Ca	8g	0	1/2	0.1082(1)	0.71(4)	8
O_1	4d	0	1/2	1/4	0.79(11)[a]	4
O_2	4e	0	0	0.1367(9)	0.79(11)[a]	4
O_3	4e	0	0	0.6309(9)	0.79(11)[a]	4
C	2a	0	0	0	3.1(9)	2
O_4	16l	0.163(6)	0.236(8)	0	1.6(8)	4
O_5	8i	0	0.24(1)	0	4.5(9)	2

[a] The thermal parameters of O_1, O_2, and O_3 were constrained.

XRD study. In order to try to localize the carbonate ions, the structure of this new phase was investigated from the intensities of the first 141 reflections on the powder XRD pattern. The reflection conditions observed on the ED patterns for the 5 × 5 × 18 Å^3 cell indicate eight possible space groups: *I4/mmm*, *I*-42*m*, *I*-4*m*2, *I*4*mm*, *I*422, *I*4/*m*, *I*-4, and *I*4. Due to the fact that the Patterson function does not depend on the space group, models can be proposed by considering the interatomic vectors deduced from the Patterson maps. According to the choice of the origin in the cell, four slightly different models can be proposed, corresponding to the atomic coordinates of calcium and thallium listed in Table 3. Fourier difference series allowed the oxygen atoms of the CaO and TlO layers to be located without ambiguity (Table 2). In any case, the variations of the atomic positions are small; thus the four models do not differ fundamentally from one another. Nevertheless, the HREM observations that imply a translation of two successive oxygen–carbonate layers suggest that the fourth model is closer to reality. Considering the most symmetric space group *I4/mmm*, refinements of the atomic coordinates of the metal atoms, the oxygen atoms, and the thermal factors of Tl and Ca were carried out successively. Then Fourier difference series were studied in order to locate the additional oxygen atoms or carbonate groups. The section at y = 1/4 along the **c** direction clearly shows a residual electronic density, split over at least two positions along **a**, that indicates the presence of oxygen (Fig. 8, top). On the section at z = 0 (Fig. 8, bottom), one observes rather diffuse and elongated electronic densities at 0.2, 0.2, 0,

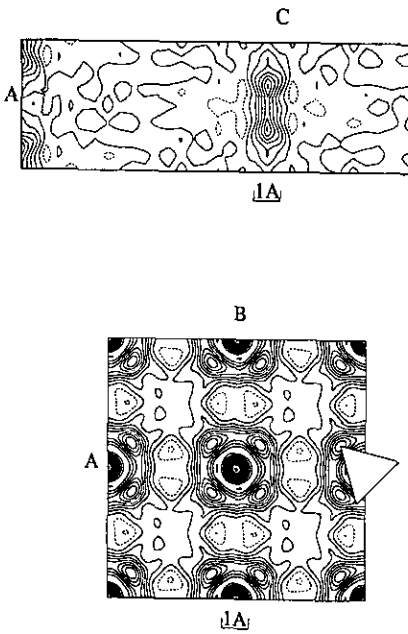

FIG. 8. Fourier difference maps after the refinement of the atomic positions in model IV (see Table 2). (top) Section at $y = 1/4$ in the (x,z) plane. (bottom) Section at $z = 0$ in the (x,y) plane. Four cells are drawn for convenience and a schematic carbonate group is displayed at the right scale.

and sharper residual electronic density at 0, 0, 0. These maps strongly suggest that the carbon atom is located at the origin, whereas the oxygen atoms forming the CO_3^{2+} group are all sitting in the $z = 0$ plane. The interatomic distances forming such a CO_3^{2-} group (Fig. 8, bottom) are compatible with the geometry of the carbonate group. Nevertheless it was noted that there are many possible orientations of the carbonate groups within the (001) plane due to the fourfold symmetry of the space group. Note also that these observations corroborate the HREM results, since on carbonate group of one layer is related to the carbonate group of the next layer by a 1/2, 1/2, 1/2 translation; it is also compatible with the fact that there is only one CO_3^{2-} group per layer for two thallium or calcium ions per layer as shown by HREM. The final refinement of atomic positions led to good reliability factors in spite of the poorly defined oxygen positions of the carbonate groups. The final atomic positions are given in Table 3 and Fig. 9 shows the X ray profiles.

DISCUSSION

This study shows that the structure of the oxycarbonate $Ca_4Tl_2CO_3O_6$ (Fig. 10a) can be described as built up from rock salt-type layers $[Ca_2TlO_3]_\infty$ interleaved with carbonate layers located between two successive $[CaO]_\infty$ layers. Interesting is the orientation of the CO_3^{2-} groups,

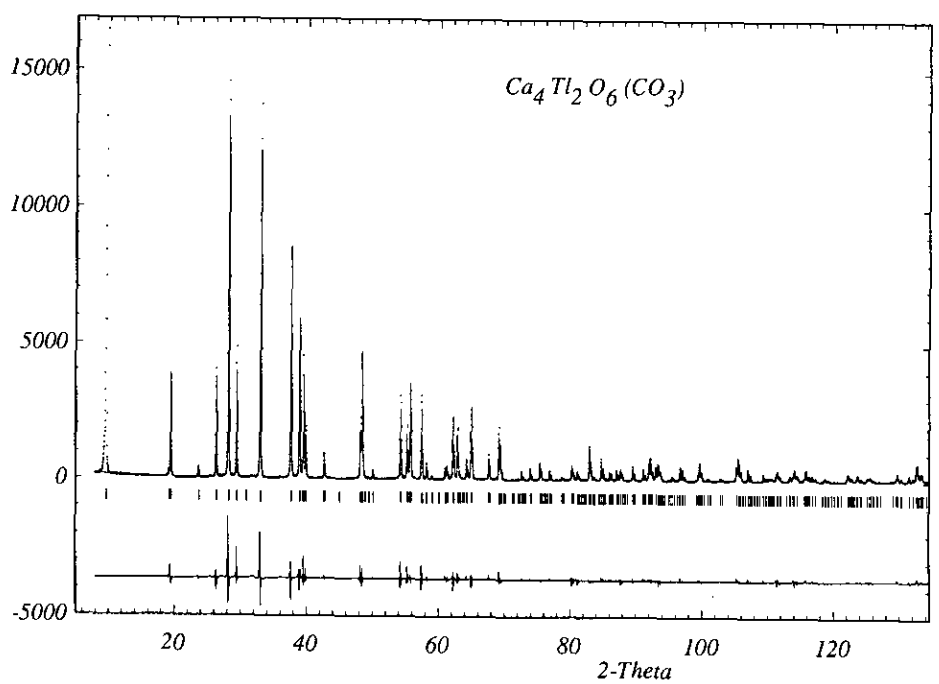

FIG. 9. Rietveld refinement profile of the X ray powder diffraction data for $Ca_4Tl_2O_6CO_3$. The observed (dots), calculated (continuous line), and difference profiles (bottom line) are shown. The vertical marks show positions calculated for Bragg reflections. The first Bragg peak is not refined because, at this angle, the cross section of the sample is lower than the X ray beam dimensions.

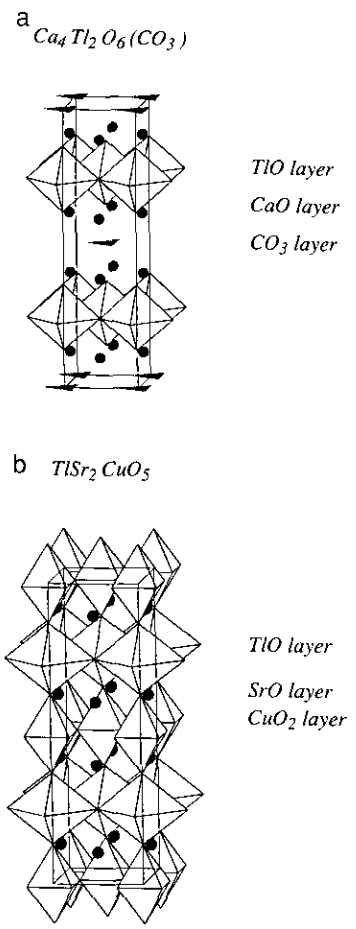

FIG. 10. (a) Crystal structure of $Ca_4Tl_2O_6CO_3$. (b) Crystal structure of $TlSr_2CuO_5$. The outline cell does not refer to the true cell of $TlSr_2CuO_5$.

whose plane is parallel to the rock salt layers, contrary to the copper oxycarbonates such as $Sr_2CuO_2CO_3$ (5) or $Tl_{0.5}Pb_{0.5}Sr_4Cu_2CO_3O_7$ (1) where the CO_3^{2-} planar group are oriented orthogonally to the perovskite layers. The interatomic distances observed for this phase (Table 4) are close to those usually observed for thallium and calcium oxides. The octahedral coordination of thallium is rather distorted with four long basal Tl–O distances of 2.39 Å, and two shorter ones of 2.11 Å. This coordination, usually found for Tl(III) in many oxides, is different from the square planar coordination observed for this element in $Sr_4Tl_2O_7$ (3). Moreover the calculated valence for thallium of 2.92 using Altermatt and Brown parameters (6) is in good agreement with the trivalent character of thallium, to be compared to 2.1 in $Sr_4Tl_2O_7$.

TABLE 4
Some Interatomic Distances in $Ca_4Tl_2CO_3O_6$

$Tl–O_1$	2.390(1) Å × 1
$Tl–O_2$	2.11(2) Å × 1
$Tl–O_3$	2.12(2) Å × 1
$Ca–O_1$	2.580(2) Å × 1
$Ca–O_2$	2.445(3) Å × 2
$Ca–O_3$	2.425(3) Å × 2
$Ca–O_4$	2.47(2) Å × 1
$Ca–O_5$	2.32(3) Å × 1

Note that the structure of the oxycarbonates $A_4Tl_2CO_3O_6$ is closely related to that of the "1201" cuprates TlA_2CuO_5 (7, 8), with A = Sr, Ba (Fig. 10b). In both structures one recognizes similar distorted rock salt layers $[A_2TlO_3]$ with A = Ca, Sr, Ba. The $[CuO2]_\infty$ layers of square planar groups in TlA_2CuO_5 (Fig. 10b) are replaced by layers of carbonate groups in the oxycarbonates $A_4Tl_2CO_3O_6$ (Fig. 10a).

CONCLUDING REMARKS

This study shows the great ability of thallium oxycarbonates to adopt a layer structure. The close relationships with the "1201" thallium cuprates TlA_2CuO_5 explains the existence of numerous thallium cuprates within a layer structure and suggests the possibility to generate new thallium copper oxycarbonates with closely related structures. The close relationships of the oxycarbonates $A_4Tl_2CO_3O_6$, with the oxide $Sr_4Tl_2O_7$ discovered several years ago by Schenck and Müller-Buschbaum (3) raises the issue of the stability of the latter oxide and of its possible total, or partial, carbonation.

The XRD and HREM results described here for $Ca_4Tl_2CO_3O_6$ give only an average picture of the real structure. There is no doubt that the latter should be better described in a less symmetric space group than *I4/mmm*. Such a study cannot be reasonably carried out from powder XRD data due to the small scattering of light atoms (C,O). A complete neutron diffraction study will be performed in order to understand the orientation of the CO_3^{2-} groups in the structure.

REFERENCES

1. M. Huve, C. Michel, A. Maignan, M. Hervieu, C. Martin, and B. Raveau, *Physica C* **205**, 219(1993).
2. F. Goutenoire, M. Hervieu, A. Maignan, C. Michel, C. Martin, and B. Raveau, *Physica C* **210**, 359(1993).
3. R. V. Schenck, H. Müller-Buschbaum, *Z. Anorg. Allg. Chem.* **396**, 113(1973).
4. J. Rodriguez-Carjaval, *in* "Proceeding Satellite Meeting on Powder Diffraction of the XVth Congress of International Union of Crystallography, Toulouse, France, July 1990.
5. M. Uehara, S. Sahota, H. Nakata, J. Akimitsu, and Y. Matsui, *Physica C* **222**, 27(1994).
6. I. D. Brown and D. Altermatt, *Acta Crystallog. B* **41**, 244(1985).
7. S. S. Parkin, V. Y. Lee, A. I. Nazzal, R. Savoy, R. Beyers, and S. J. LaPlaca, *Phys. Rev. Lett.* **61**, 750(1988)
8. J. S. Kim, J. S. Swinnea, and H. Steinfink, *J. Less-Common Metals* **156**, 347(1989).